Supporting Information for:

Desolvation Induced Crystal Jumping: Reversible Hydration and Dehydration of Spironolactone-Saccharin Cocrystal with Water as Jumping-Mate

Yifu Chen,[1,2] Bo Jing,[1,2] Zewei Chang,[1,2] and Junbo Gong,[1,2]*

[1] State Key Laboratory of Chemical Engineering, School of Chemical Engineering and Technology, Tianjin University, Weijin Road 92, Tianjin 300072, China.

[2] Collaborative Innovation Center of Chemical Science and Engineering, Weijin Road 92, Tianjin 300072, China.

*To whom correspondence should be sent: junbo_gong@tju.edu.cn.

CrystEngComm

Author Contributions:

Y.C. conceptualized the project, directed the study, determined the experimental methods, completed the pre-experiment, analyzed and discussed the results, wrote the manuscript and drew all the figures. Under the supervision of Y.C., B.J. and Z.C. prepared the samples, performed most of the experiments and characterization, and organized the sup-porting information. C.Y. and B.J. contributed equally to this work. J.G. acquired funding for the whole study. All authors commented on the manuscript.

Supplement Files Involve:

- **A PDF File** (Supplementary text with experimental information, figures and tables)
- **Movies**

- Movie for jumping behavior of SPI-SAC cocrystal hydrate (Movie_S1.MP4)
- Another Movie for jumping behavior of SPI-SAC cocrystal hydrate (Movie_S2.MP4)
- Movie for recyclable jumping of SPI-SAC cocrystal hydrate (Movie_S3.MP4)
- Movie for multiple jumping of SPI-SAC cocrystal hydrate (Movie_S4.MP4)

- **Crystallographic Data**

- Hemihydrate SPI-SAC-0.5H_2O at 113 K, CCDC 2067403 (Cif_1.cif)
- Hemihydrate SPI-SAC-0.5H_2O at 298 K, CCDC 2070184 (Cif_2.cif)
- Quarterhydrate SPI-SAC-0.25H_2O at 353 K, CCDC 2070185(Cif_3.cif)
- Anhydrate SPI-SAC at 393 K, CCDC 2070186(Cif_4.cif)
- 1/8 hydrate SPI-SAC-0.125H_2O at 298 K, CCDC 2070187(Cif_5.cif)

List of Contents

Chemicals and Instruments

All reagents were commercially available and used as received without further purification. Spironolactone (SPI, 99%) and Saccharin (SAC, 99%) was purchased from Heowns. Isopropanol (99.5%) was purchased from Shanghai Meryer Chemical Technology. All water used in our experiments is distilled water.

The X-ray powder diffraction (XRD) data were collected using a Rigaku D/max 2500. The X-ray single crystal diffraction (XRSD) data was collected on single-crystal X-ray diffractometer (Rigaku 007, Saturn 70). The thermogravimetric analyzer (TGA) was recorded using TGA/DSC system (Mettler-Toledo, 1 STAR^e). The differential scanning calorimetry (DSC) was carried out on a DSC 1 STAR^e system (Mettler-Toledo, 1 STAR^e). The videos and micrographs of jumping crystals were recorded using a microscope (Nikon SMZ745T) with a camera. In the process of material preparation, the temperature & humidity control chamber (ESPEC, GPR-2) was used for storing crystals. The vacuum oven (Taisite, DZ-2BC II) was used to dehydrate the crystals completely. Weighing and gravimetric analysis were carried out on a five digit balance, up to 0.01 mg (Mettler-Toledo, ML204T/02).

Detailed Experimental Procedures

1. Preparation of SPI-SAC cocrystal hydrates: For getting crystal seeds, a mixture of 40 mg (around 0.10 mmol) of SPI and 18 mg (around 0.10 mmol) of SAC was ground using a mortar for 5 min and then was ground for another 5 min after adding 40 μL of water. SPI (208 mg, 0.50 mmol) and SAC (92 mg, 0.50 mmol) were dissolved well in 10 mL isopropanol at 353 K. After adding 10 mL of water, the solution was cooled to room temperature without crystallization. After adding little seeds, the solution was kept to evaporate solvent slowly for about 2 days to obtain colorless SPI-SAC cocrystal hydrates (Figure S1).

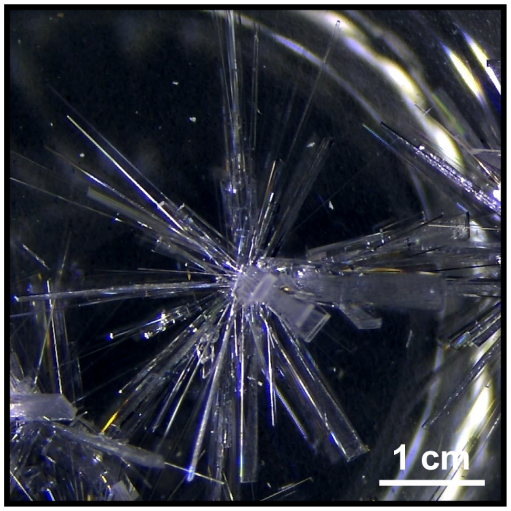

Figure S1. Microphotographs of prepared SPI-SAC cocrystal hydrates.

2. Preparation of SPI-SAC cocrystal hydrates with different water content: The crystals were quickly fished out from saturated solution to a culture dish and stored in the GPR-2 for 12 h. The crystals with different water content were obtained by controlling the temperature and relative humidity (RH) of the air in the GPR-2 (Figure S2, Table S1). The water content was calculated with the difference of sample weight before and after vacuum drying divided by the initial sample weight (averaged and statistically analyzed from three parallel groups of each sample), which was also confirmed by TGA (Figure S7, S8). Additionally, the reloading water process of anhydrate SPI-SAC crystals was carried out in the GPR-2 at 90% RH, 298 K for 12 h.

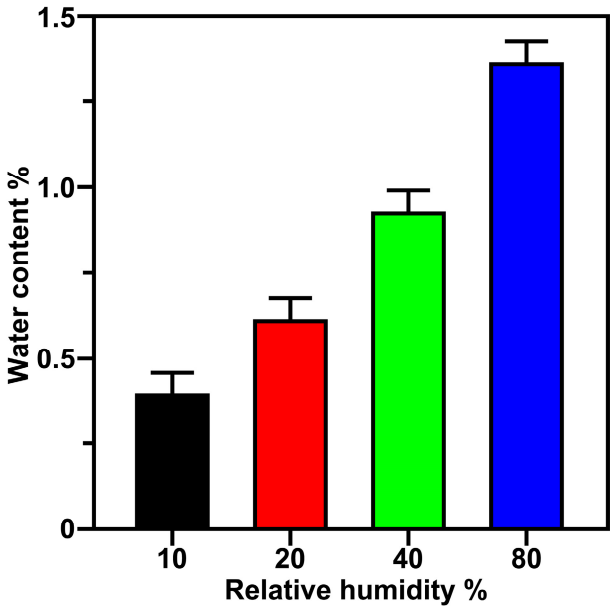

Figure S2. Water content of SPI-SAC cocrystal hydrates under different relative humidity.

3. Observation of the jumping behavior of SPI-SAC cocrystal hydrates: Some prepared SPI-SAC cocrystal hydrates were selected to be put on glass slide and heated on an open temperature-controlled hot stage (ZNCL-BS140, Tianjin Xingke Instrument Co., Ltd.) from 298 K to 353 K with the average heating rate 18.3 K/min, and observed under the microscope. To ensure the continuity and integrity of the crystal motions, we recorded the video of the crystals heating process and took screenshots from the video (Movie S1).

Notes: Some obvious jumping behaviors including multiple jumping were shown in Figure S10, S11 and Supplement Movie S2, S4.

4. Observation of the recyclable jumping behavior of SPI-SAC cocrystal hydrates after solvent reloading: During the first heating from 298 K to 353 K, average heating rate 10 K/min, some crystals were separated from hot stage in time after jumping, and placed in the wet air (298 K, 90% RH) kept by the GPR-2 for 6 h to reload water. Then we reheated them under the same heating conditions to observe jumping behavior. The heating and reloading water process was repeated until some of jumped crystals jumped again. All the jumping processes were recorded by the camera of the microscope (Movie S3).

Notes: We have done heating and reloading water cycles many times for crystals, some of them could still jump three times in total showing good reversibility so we didn't do further experiments.

X-Ray Powder Diffraction Patterns

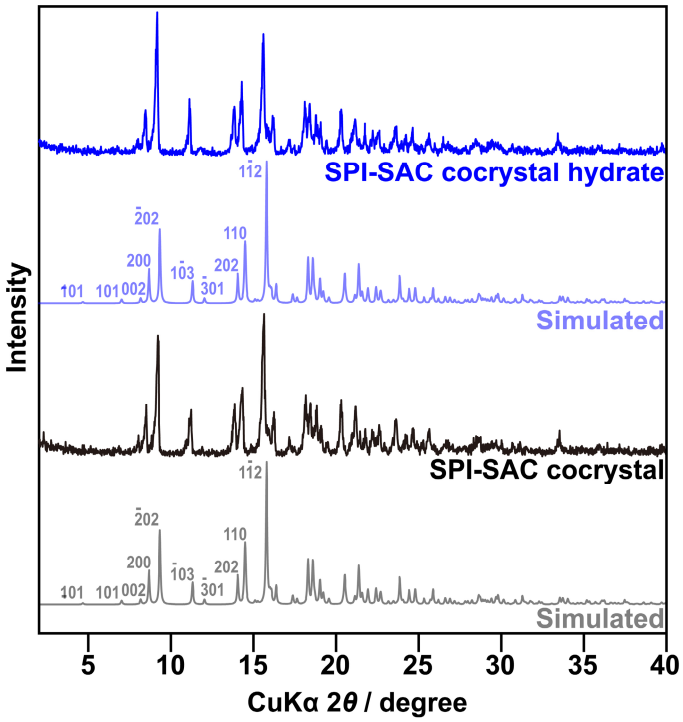

Figure S3. X-ray Powder Diffraction Patterns patterns of SPI-SAC cocrystal hydrate powders and SPI-SAC cocrystal powders after complete dehydration and corresponding simulated crystallographic diffraction patterns from single crystal structure (CCDC 2070184, CCDC 2070186, respectively). Noting that the lattice parameters were almost unaffected by the introduction or removal of the water molecule.

Differential Scanning Calorimetry Analysis

DSC analysis were carried out on powder sample, single crystals of the SPI-SAC cocrystal hydrates and SPI-SAC cocrystal anhydrate single crystals prepared by vacuum drying at 393 K. All the heating and cooling rate was 10 K/min.

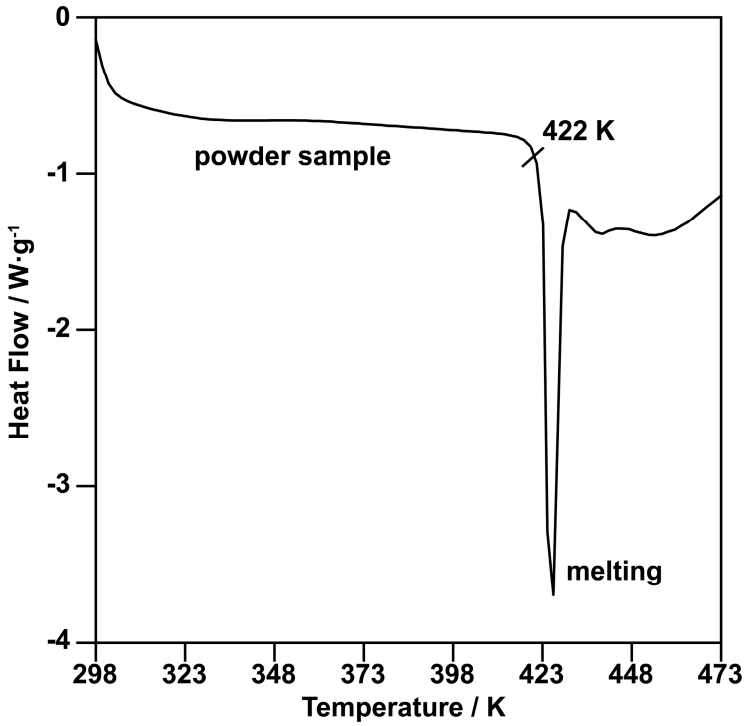

Figure S4. DSC curve of SPI-SAC cocrystal

. Heating rate was 10 K/min. The onset of the melting of SPI-SAC cocrystal hydrates was 422 K.

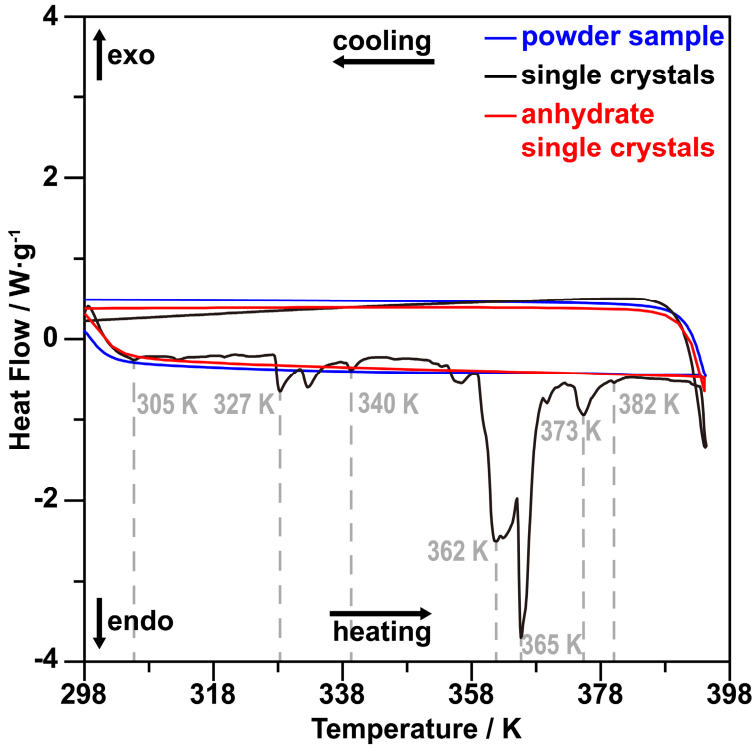

Figure S5. DSC curves of SPI-SAC cocrystal hydrates powder samples, single crystals, and SPI-SAC anhydrate single crystals under a thermal cycling. Heating and cooling rate was 10 K/min.

Notes: (1) The sawtooth profile was the common signature of crystal jumping and these sawtooth profiles appearing from 305 K to 382 K along with continuous dehydration of SPI-SAC cocrystal hydrates indicates intermittent jumping happened in SPI-SAC cocrystal hydrates. (2) The endothermic peak was not observed in anhydrate crystals, suggesting that crystals could not jump after the complete desolvation.

Thermogravimetric Analysis

The powder samples and single crystals of SPI-SAC cocrystal hydrates were performed TGA to confirm temperature range of water loss (Figure S6).

In order to study the effect of the jumping-mate (water) content on crystal jumping behavior, single crystals of SPI-SAC hydrates with different water contents were prepared in the GPR-2 with different temperature and relative humidity (Figure S2, Table S1) and performed TGA (Figure S7). The jumping parameters of the SPI-SAC-xH_2O with different water content were also shown in Table S2.

To confirm the reversible loading water process, TGA was also performed on SPI-SAC cocrystal anhydrates (single crystals) after being placed in the wet air for 12 h (Figure S8).

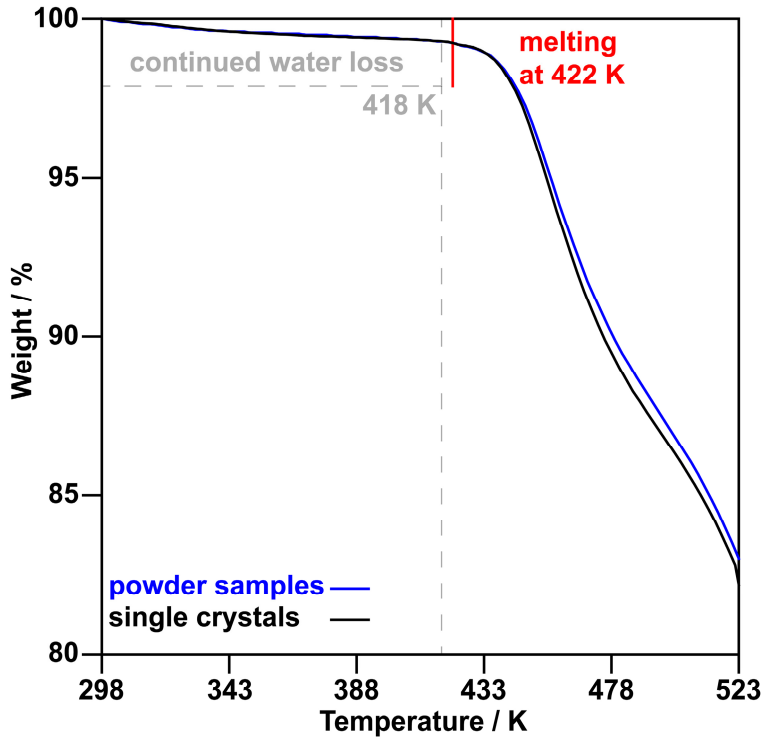

Figure S6. TGA curves of SPI-SAC cocrystal hydrates for single crystals and powder samples. Heating rate was 10 K/min. The decline of the curve from 298 K to 418 K indicated continuous water loss during the heating process.

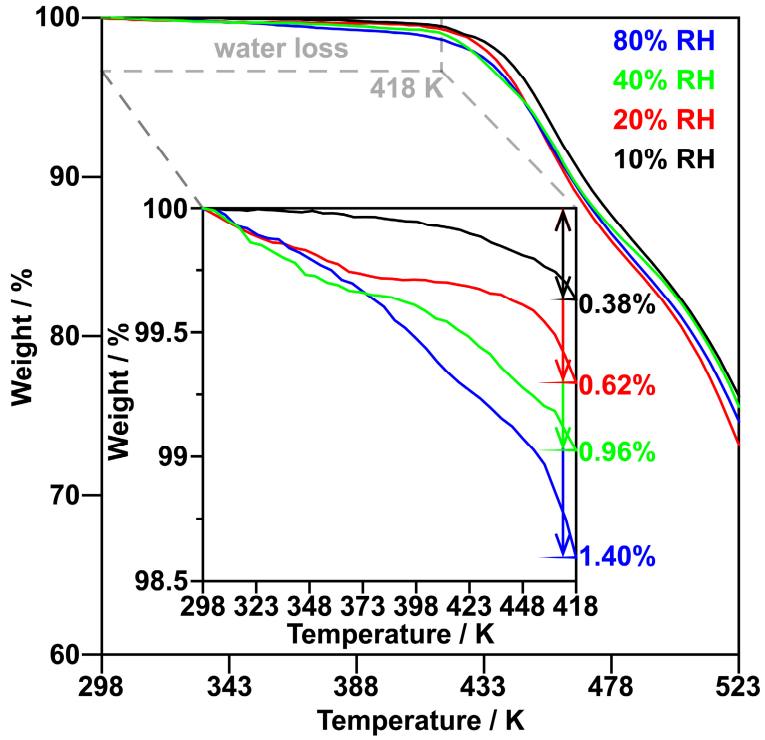

Figure S7. TGA curves of SPI-SAC cocrystal hydrates (single crystals) with different water content.

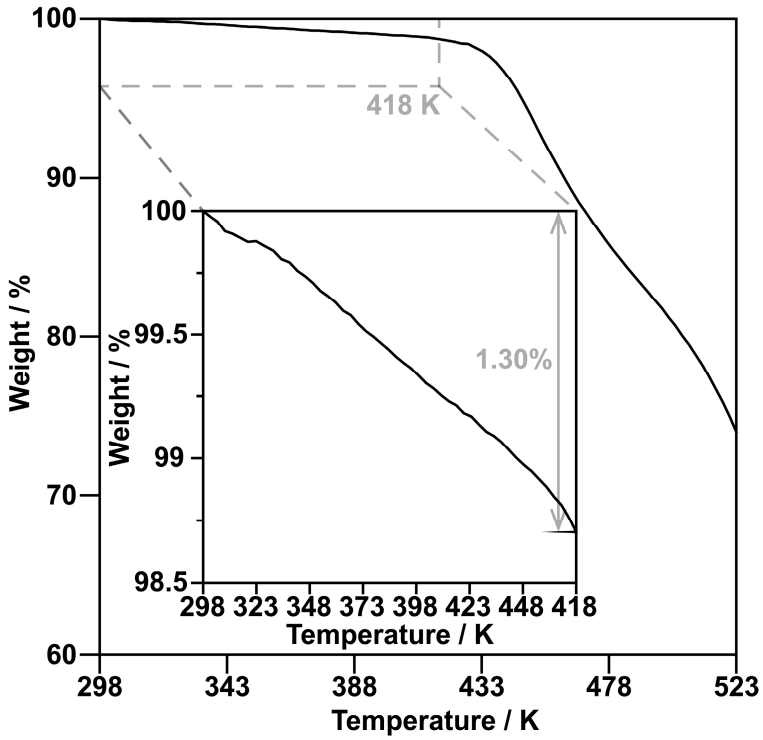

Figure S8. TGA curves of SPI-SAC cocrystal anhydrates (single crystals) after being placed at 90% RH, 298 K for 12 h to reload water.

Notes: The water loss of 1.30% indicated the release-reloading water process is reversible.

Comparison of Jumping Parameters

The jumping experiments of SPI-SAC cocrystal hydrates with different water content (Table S1) were carried out for comparison. We measured the length, width and height of the crystals, but it is difficult to obtain the height/thickness of crystals accurately, especially for thinner crystals. Their thicknesses were estimated. The weight of every kind crystal before and after jumping and the jumping temperature of every crystal are recorded. Besides, crystals jumping were recorded by stereomicroscope and phone camera simultaneously for the jumping distance and jumping height. The jumping height is measured with a ruler placed perpendicularly near the heating stage. The horizontal jumping distance is obtained by measuring the distance in a straight line between the position before and after jumping of the crystal. The speeds of the jumping, including horizontal speeds and vertical speeds, are equal to jumping distances divided by time, in which the jumping time is calculated by multiplying the number of frames difference before and after jumping and the time interval of each frame (0.01 s) in the video. Reversibility is whether the crystal can return to its original state by heating or placed in the wet air. The maximum number of cycles is measured by counting the number of heating and reloading water circle until crystals cannot jumping anymore while heating. We have done cycles many times for every kind of crystal, some of them could still jump three times in total showing good reversibility so we didn't do further experiments while recorded the maximum number 3 of cycles uniformly. The maximum jumping frequency of a single crystal is the maximum number of jumps counted during a

heating process. Jumping probability is ratio of the number of jumping crystals to the number of all crystals for one kind jumping crystal in all experiments (Table S2).

Table S1. Water content of SPI-SAC cocrystal hydrates under different storage conditions.

Water content	(1.45±0.09)%	(1.36±0.09)%	(0.92±0.1)%	(0.61±0.08)%	(0.39±0.07)%
Temperature	298 K	298 K	298 K	298 K	298 K
RH	90%	80%	40%	20%	10%

Table S2. Comparison of the jumping parameters of the SPI-SAC-xH_2O with different water content.

Jumping Parameters	SPI-SAC-0.46H_2O	SPI-SAC-0.32H_2O	SPI-SAC-0.19H_2O	SPI-SAC-0.13H_2O
Crystal Length/cm	0.05-0.5	0.05-0.5	0.05-0.5	0.05-0.5
Crystal Width/cm	0.02-0.1	0.02-0.1	0.02-0.1	0.02-0.1
Crystal Height/cm	0.01-0.04	0.01-0.04	0.01-0.04	0.01-0.04
Jumping Temperature/K	298-393	298-393	298-393	298-393
Weight Difference/%	1.36	0.92	0.61	0.39
Jumping Height/cm	0.5	0.5	0.4	0.2
Jumping Distance/cm	3.3	2.8	1.6	0.5
Vertical Jumping Speed/cm·s^{-1}	5	5	4	2
Horizontal Jumping Speed/cm·s^{-1}	33	28	16	5
Reversibility	Yes	Yes	Yes	Yes
Maximum Number of Cycles	3	3	3	3
Maximum Jumping Frequency	4	3	2	2
Jumping Probability	81 in 136	71 in 146	49 in 122	28 in 115

Crystallographic Information

A single crystal of SPI-SAC-0.5H_2O was selected and fixed on a Bruker APEX-II CCD diffractometer. The crystal was kept at 298 K, 353 K, 393 K, 298 K during data collection. Using Olex2[1], the structure was solved with the ShelXS[2] structure solution program using Direct Methods and refined with the XL[2] refinement package using Least Squares minimisation. After obtaining the crystallographic information of the four crystal structure, we found that the process of loading water was reversible. All the four single crystal structure data were shared by us, could be downloaded from the Cambridge structural database, and summarized in Table S3.

Notes: (1) The tested sample was the same crystal. (2) The crystal was kept for 5 minutes to stabilize the temperature before data collection. (3) after tested at 393 K, we had a break and turned off N_2 flow. The crystal was placed in the air for 6 h at 298 K and tested again. We found the electron density of the H_2O molecule again, which indicates that the water removal/absorption process is reversible. (4) We found another crystal form of SPI-SAC cocrystal hydrate and obtained single crystal structure (CCDC 2067403). The polymorphism of SPI-SAC cocrystal hydrate was not discussed in this work.

Table S3. Crystal structure information of SPI-SAC-xH_2O with variable water content, 0.5H_2O, 0.25H_2O, 0H_2O, 0.125H_2O at different temperature.

SPI-SAC-xH_2O	SPI-SAC-0.5H_2O	SPI-SAC-0.25H_2O	SPI-SAC	SPI-SAC-0.125H_2O
CCDC	2070184	2070185	2070186	2070187
Formula	$C_{14}H_{14}N_2O_2$	$C_{14}H_{14}N_2O_2$	$C_{31}H_{37}NO_7S_2$	$C_{31}H_{37.25}NO_{7.13}S_2$
Temperature (K)	298 K	353 K	393 K	298 K
Space Group	*C*2	*C*2	*C*2	*C*2
Crystal System	monoclinic	monoclinic	monoclinic	monoclinic
a (Å)	25.2663(9)	25.2658(18)	25.208(2)	25.321(6)
b (Å)	6.3994(2)	6.3976(5)	6.3747(6)	6.4135(15)
c (Å)	22.1324(8)	22.0858(16)	21.980(2)	22.097(5)
α (deg)	90	90	90	90
β (deg)	120.7850(10)	121.1380(10)	121.0010(10)	121.404(3)
γ (deg)	90	90	90	90
V ($Å^3$)	3074.33(19)	3055.6(4)	3027.5(5)	3062.8(12)
ρ_{cal}, (Mg/m^3)	1.315	1.313	1.316	1.305
μ, (mm^{-1})	1.294	0.222	0.223	0.221
Z	4	4	4	4
R-factor	0.0396	0.1013	0.1712	0.0525
wR_2	0.1140	0.2855	0.2627	0.1288
GOF	1.066	1.058	0.934	0.991
Total no. of unique data (I>2σ(I))	8925	5144	9288	16159
Total no. of data	51668	10209	16633	8823
Number of parameters	378	381	373	375

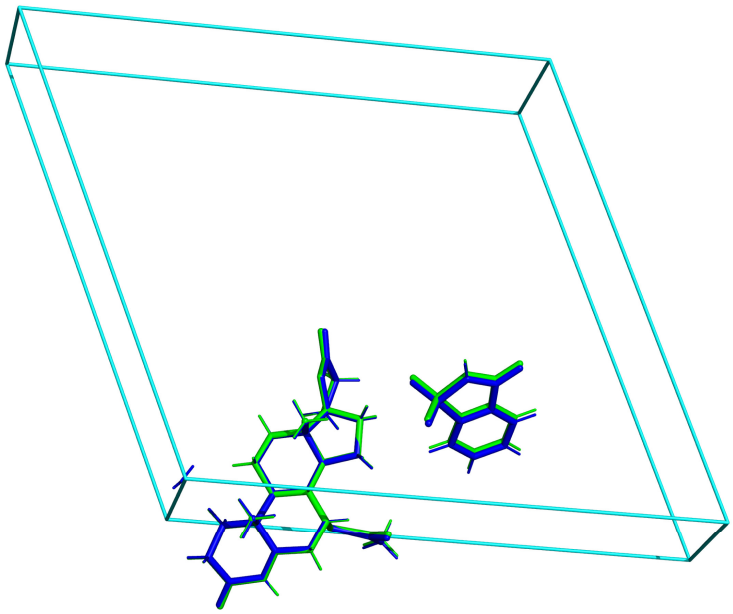

Figure S9. Overlay of the crystal structure of SPI-SAC-0.5H_2O (blue, CCDC 2070184) and SPI-SAC (green, 2070186). Noting that there was no conformational change of SPI and SAC molecule before and after dehydration.

Table S4. Comparison of the crystal system, lattice constant, and cell volume per molecule of SPI-SAC-0.5H_2O, SPI-SAC -0.25H_2O, and SPI-SAC.

SPI-SAC-xH_2O	system	a (Å), Δa (%)	b (Å), Δb (%)	c (Å), Δc (%)	α (deg), Δα (%)	β (deg), Δβ (%)	γ (deg), Δγ (%)	V/Z (Å^3), Δ(V/Z) (%)
SPI-SAC-0.5H_2O	monoclinic	25.2663, 0	6.3994, 0	22.1324, 0	90, 0	120.785, 0	90, 0	3074.33, 0
SPI-SAC-0.25H_2O	monoclinic	25.2658, 0	6.3976, 0.03	22.0858, 0.21	90, 0	121.138, -0.29	90, 0	3055.6, 0.61
SPI-SAC	monoclinic	25.208, 0.23	6.3747, 0.39	21.98, 0.69	90, 0	121.001, -0.18	90, 0	3027.5, 1.52

Notes: All the comparison is based on the crystal structure of SPI-SAC-0.5H_2O at 298 K.

Notes: The jumping behaviors in this work occurred continuously in a temperature range (298 K-393 K). The earlier jumping motions are below 320 K, and the lattice change in Δ(V/Z) should be below 0.61%.

Additional Graphs

The jumping behavior of SPI-SAC cocrystal hydrates was directly observed and recorded under the microscope with a variable-temperature stage (Figure S10, Movie S2). Some crystals were put on the stage and the initial state of them was shown in Figure 3a. Three crystals were numbered as 1, 2, 3 for convenient description. During the temperature ranging from 298 K to 393 K with the average heating rate of 10 K/min, persistent escape of solvents (water) from the surface of the crystals was observed, accompanied by the various jumping motions including jumping, flipping and swing.

For crystal 1, it jumped suddenly at 278 s, 344 K with a distance of 3 mm, and followed by little rolling (Figure S10b-f). Obvious heat-induced solvent desorption on the crystal surface could be seen, which provided as enough fuel for crystal 1 to complete the jumping action in a second. For crystal 2, and 3, they flipped at 317 s, 351 K and swung at 395 s, 364 K, respectively (Figure S10g-k). It should be noted that these small-scale jumping motions happened in crystal 2 and 3 was the frequent occurrence throughout the whole jumping experiment (Movie S2). Figure 3i showed the final state of all crystals. Besides, the DSC results of anhydrated single crystals showed disappearing sawtooth curve (Figure S5) compared to the hydrate single crystals, indicating jumping behavior did not happened in the SPI-SAC cocrystal anhydrate, which was also confirmed by us in the jumping experiment.

Another multiple jumping behavior (3 times) was recorded under the microscope (Figure S11, Movie S4). Temperature ranged from 298 K to 353 K with the average heating rate 10K/min. The crystal in Figure S11 jumped at 240 s, 342 K, and then jumped at 272 s, 347 K, finally jumped at 283 s, 349 K, 3 times in total.

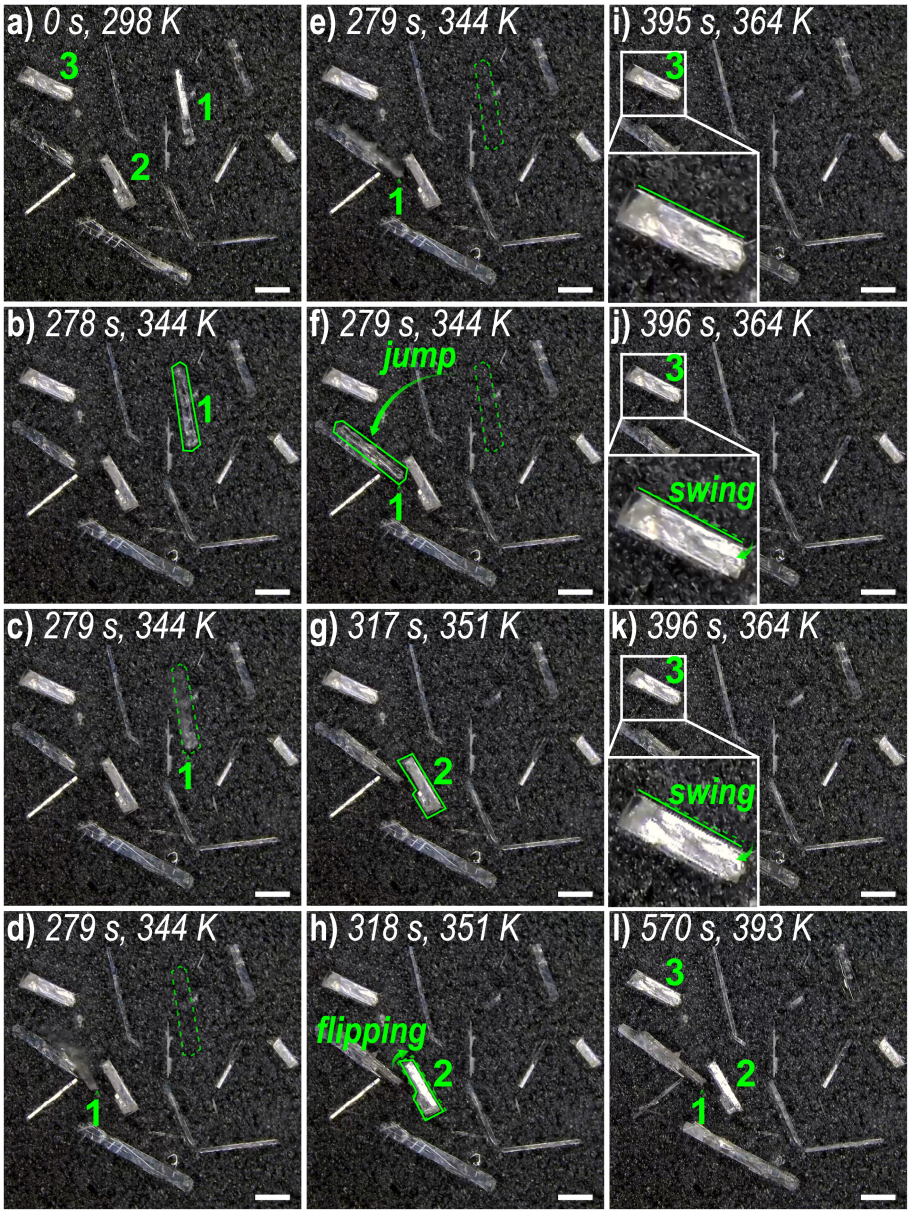

Figure S10. Microscopic observation of the jumping behavior of SPI-SAC cocrystal hydrates from 298 K to 393 K (a-l), and partial enlarged microphotographs (i, j, k, inset). Average heating rate, 10 K/min. Noting that jumping distance of crystal 1 was about 3 mm followed by little rolling, and crystal 3 swung slightly at 364 K. Scale bar, 1 mm.

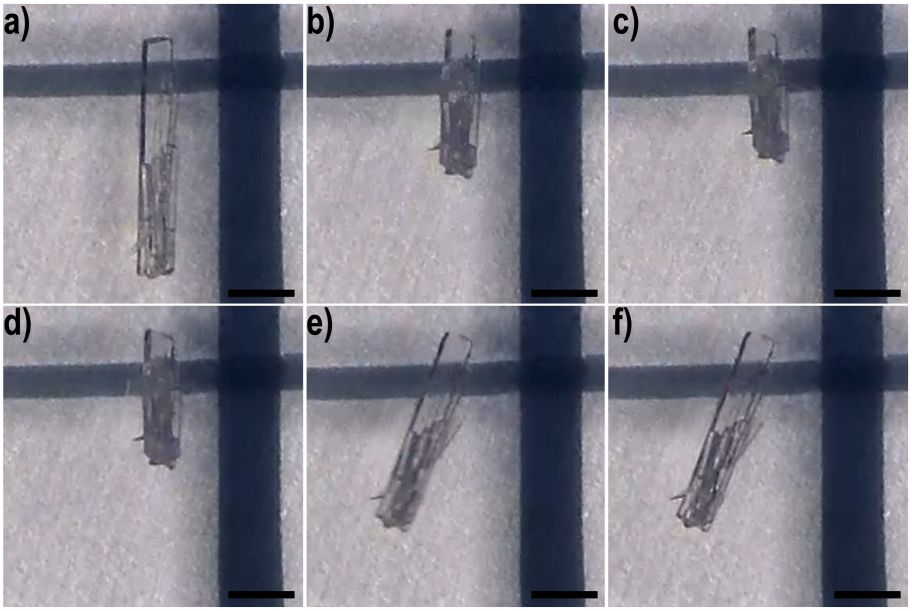

Figure S11. Microscopic observation of the multiple jumping behavior of SPI-SAC cocrystal hydrates from 342 K to 353 K (a-f). Average heating rate, 10 K/min. Noting that the crystal jumped 3 times in heating process from 342 K-353 K. Scale bar, 1 mm.

Comparison of the Unit Cell Parameters of the Reported Jumping Crystals

Table S5. Comparison of the unit cell parameters of the reported jumping crystals.

Reported cases	Δ(V/Z)	Notes
1[3]	+3.3%	a (-11.6%), b(-20.7%), c(-17.1), β(-27.4%)
2[4]	+1.8%	a(-3.1%), b(+4.4%), c(+1.3%), β(+1.4%)
3[5]	+2.4%	a(+12.4%), b(+2.0%), c(−12.2%), β(-5.8%)
4[6]	+3.0%	a(+0.8%), b(+10.5%), c(−7.5%)
5[7]	+1.1%	a(−20.0%), b(+20.6%), c(−25.3%), α(+6.7%), β(−18.9%), γ(−8.5%)
6[8]	+4.3%	a(+8.8%), b(+12.3%), c(−14.8%)
7[9]	+0.7%	a(+1.4%), b(−1.6%), c(+0.7%)
8[10]	+3.6%	a(-1.1%), b(+1.7%), c(1.2%), β(-5.0%)
9[11]	+2.6%	a(+0.6%), c(+2.8%)
10[12]		a(+8.1%), b(-6.3%), c(-1.1%), conformation change
11[13]	-0.8%	a(+2.1%), b(+4.2%), c(-0.7%), β(+11.2%)
12[14]	-2.2%	a(−27.0%), b(-38.8%), c(+19.3%), α(+25.6%), β(−3.3%), γ(+6.1%)
13[15]	-1.4%	a(-1.0%), conformation change
14[16]	-3.6%	b(-2.2%), c(-1.6%)
15[17]	-5.3%	a(-6.4%), b(+1.9%), c(-0.6%)
16[18]	-7.3%	a(+43.5%), b(+26.7%), c(+3.5%), α(-1.04%), β(+14.4%), γ(-11.1%)
17[19]	-1.6%	a(-0.6%), b(-0.3%), c(-0.7%)
18[20]	+1.9%	a(+1.2%), c(+0.6%), β(+0.8%), conformation change
19[20]	+1.6%	a(+1.0%), b(+0.7%), conformation change
20[20]	+2.0%	b(+1.8%), conformation change
21[21]	-2.2%	a(+1.9%), b(-5.6%), c(0.9%), β(-2.8%), conformation change
22[22]	-4.1%	a(-27.2%), b(-38.9%), c(+19.8%), α(+27.4%), β(-1.7%), γ(+6.5%)
23[23]	-7.4%	a(+4.4%), b(-5.6%), c(2.7%), α(18.1%), β(31.9%), γ(+5.6%)
24[24]	+3.0%	a(-12.0%), b(+45.8%), c(+60.6%), α(7.5%), β(3.9%), γ(-5.8%)
25[24]	+4.9%	a(-11.1%), b(4.3%), c(12.9%), α(12.2%), β(3.7%), γ(-14.5%)
26[24]	+3.1%	a(+2.1%), c(+1.0%)
27[25]	+2.1%	a(+7.7%), b(-4.6%), c(-0.8%)
28[25]	+1.0%	a(+4.8%), b(-3.2%), c(-0.8%), β(-2.1%)

29[26]	+1.7%	a(-25.0%), b(+20.9%), c(+5.6%), α(+15.2%), β(+6.5%), γ(+2.0%)
30[27]	-3.0%	a(-4.2%), b(-11.5%), c(8.3%), α(13.0%), β(1.0%), γ(8.2%)
31[27]	+0.9%	a(+1.7%), b(−1.4%), c(+0.6%)
32[27]	+0.5%	a(-51.1%), b(−31.8%), c(+0.6%)
33[28]	+0.9%	a(-2.8%), b(+1.7%), α(-12.5%), β(+4.3%), γ(-4.8%)
34[29]	-2.3 %	a(-4.2%), c(+1.2%), α(+9.6%), β(+6.6%), γ(+25.7%)
35[30]		Not single-crystal-to-single-crystal

Notes: The reported data without single crystal structure information before and after jumping as well as the calculated values from powder X-ray diffraction were not in this table.

References

(1) Dolomanov, O. V.; Bourhis, L. J.; Gildea, R. J.; Howard, J. A. K.; Puschmann, H. OLEX2: A Complete Structure Solution, Refinement and Analysis Program. *J. Appl. Crystallogr.* **2009**, *42*, 339-341.

(2) Sheldrick, G. M. A Short History of SHELX. *J. Appl. Crystallogr.* **2008**, *64*, 112-122.

(3) Etter, M. C.; Siedle, A. R. Solid-State Rearrangement of (Phenylazophenyl) Palladium Hexafluoroacetylacetonate. *J. Am. Chem. Soc.* **1983**, *105*, 641-643.

(4) Lieberman, H. F.; Davey, R. J.; Newsham, D. M. T. Br···Br and Br···H Interactions in Action: Polymorphism, Hopping, and Twinning in 1,2,4,5-Tetrabromobenzene. *Chem. Mat.* **2000**, *12*, 490-494.

(5) Steiner, T.; Hinrichs, W.; Saenger, W.; Gigg, R. Jumping Crystals': X-ray Structures of the Three Crystalline Phases of (±)-3,4-Di-*O*-acetyl-1,2,5,6-Tetra-*O*-benzyl-*myo*-inositol. *Acta Crystallogr. Sect. B-Struct. Sci.Cryst. Eng. Mat.* **1993**, *49*, 708-718.

(6) Skoko, Ž.; Zamir, S.; Naumov, P.; Bernstein, J. The Thermosalient Phenomenon. "Jumping Crystals" and Crystal Chemistry of the Anticholinergic Agent Oxitropium Bromide. *J. Am. Chem. Soc.* **2010**, *132*, 14191–14202.

(7) Davey, R. J.; Maginn, S. J.; Andrews, S. J.; Black, S. N.; Buckley, A. M.; Cottier, D.; Dempsey, P.; Plowman, R.; Rout, J. E.; Stanley, D. R.; Taylor, A. Morphology and Polymorphism of Terephthalic Acid. *Mol. Cryst. Liquid Cryst.* **2006**, *242*, 79-90.

(8) Centore, R.; Jazbinsek, M.; Tuzi, A.; Roviello, A.; Capobianco, A.; Peluso, A. A Series of Compounds Forming Polar Crystals and Showing Single-Crystal-to-Single-Crystal Transitions between Polar Phases. *CrystEngComm* **2012**, *14*, 2645-2653.

(9) Wu, H.; West, A. R. Thermally-Induced Homogeneous Racemization, Polymorphism, and Crystallization of Pyroglutamic Acid. *Cryst. Growth Des.* **2011**, *11*, 3366-3374.

(10) Gaztañaga, P.; Baggio, R.; Halac, E.; Vega, D. R. Thermal, Spectroscopic and Structural Analysis of a Thermosalient Phase Transformation in Tapentadol Hydrochloride. *Acta Crystallogr. Sect. B-Struct. Sci.Cryst. Eng. Mat.* **2019**, *75*, 183-191.

(11) Mei, L.; An, S. W.; Hu, K. Q.; Wang, L.; Yu, J. P.; Huang, Z. W.; Kong, X. H.; Xia, C. Q.; Chai, Z. F.; Shi, W. Q. Molecular Spring-like Triple-Helix Coordination Polymers as Dual-Stress and Thermally Responsive Crystalline Metal-Organic Materials. *Angew. Chem. Int.Ed.* **2020**, *59*, 16061-16068.

(12) Takeda, T.; Ozawa, M.; Akutagawa, T. Jumping Crystal of a Hydrogen-Bonded Organic Framework Induced by the Collective Molecular Motion of a Twisted π System. *Angew. Chem. Int.Ed.* **2019**, *58*, 10345-10352.

(13) Alimi, L. O.; Van Heerden, D. P.; Lama, P.; Smith, V. J.; Barbour, L. J. Reversible Thermosalience of 4-aminobenzonitrile. *Chem. Commun.* **2018**, *54*, 6208-6211.

(14) Lusi, M.; Bernstein, J. On the Propulsion Mechanism of "Jumping" Crystals. *Chem. Commun.* **2013**, *49*, 9293-9295.

(15) Seki, T.; Mashimo, T.; Ito, H.Anisotropic Strain Release in a Thermosalient Crystal: Correlation between the Microscopic Orientation of Molecular Rearrangements and the Macroscopic Mechanical Motion. *Chem. Sci.* **2019**, *10*, 4185-4191.

(16) Ohtani, S.; Gon, M.; Tanaka, K.; Chujo, Y. A Flexible, Fused, Azomethine-Boron Complex: Thermochromic Luminescence and Thermosalient Behavior in Structural Transitions between Crystalline Polymorphs. *Chem. Eur. J.* **2017**, *23*, 11827-11833.

(17) Martins, F. F.; Joseph, A.; Diogo, H. P.; Minas da Piedade, M. E.; Ferreira, L. P.; Carvalho, M. D.; Barroso, S.; Romão, M. J.; Calhorda, M. J.; Martinho, P. N. Irreversible Magnetic Behaviour Caused by the Thermosalient Phenomenon in an Iron(III) Spin Crossover Complex. *Eur. J. Inorg. Chem.* **2018**, 2976-2983.

(18) Shibuya, Y.; Itoh, Y.; Aida, T. Jumping Crystals of Pyrene Tweezers: Crystal-to-Crystal Transition Involving π/π-to-CH/π Assembly Mode Switching. *Chem. Asian J.* **2017**, *12*, 811-815.

(19) Seki, T.; Mashimo, T.; Ito, H. Crystal Jumping of Simple Hydrocarbons: Cooling-Induced Salient Effect of Bis-, Tri-, and Tetraphenylethene through Anisotropic Lattice Dimension Changes without Thermal Phase Transitions. *Chem. Lett.* **2020**, *49*, 174-177.

(20) Rawat, H.; Samanta, R.; Bhattacharya, B.; Deolka, S.; Dutta, A.; Dey, S.; Raju, K. B.; Reddy, C. M. Thermosalient Forms: Carryover of Thermosalient Behavior of Coformers from Single Component to Multicomponent Forms? *Cryst. Growth Des.* **2018**, *18*, 2918-2923.

(21) Takahashi, Y.; Kondo, T.; Yokokura, S.; Takehisa, M.; Harada, J.; Inabe, T.; Matsushita, M. M.; Awaga, K. Electric and Thermosalient Properties of a Charge-Transfer Complex Exhibiting a Minor Valence Instability Transition. *Cryst. Growth Des.* **2020**, *20*, 4758-4763.

(22) Nauha, E.; Naumov, P.; Lusi, M. Fine-Tuning of a Thermosalient Phase Transition by Solid Solutions. *CrystEngComm* **2016**, *18*, 4699-4703.

(23) Singh, M.; Bhandary, S.; Bhowal, R.; Chopra, D. Observation of Bending, Cracking and Jumping Phenomena on Cooling and Heating of Tetrahydrate Berberine Chloride Crystals. *CrystEngComm* **2018**, *20*, 2253-2257.

(24) Mittapalli, S.; Perumalla, D. S.; Nangia, A. Mechanochemical Synthesis of N-salicylideneaniline: Thermosalient Effect of Polymorphic Crystals. *IUCrJ* **2017**, *4*, 243-250.

(25) Mittapalli, S.; Perumalla, D. S.; Nanubolu, J. B.; Nangia, A. Thermomechanical Effect in Molecular Crystals: The Role of Halogen-Bonding Interactions. *IUCrJ* **2017**, *4*, 812-823.

(26) Karothu, D. P.; Weston, J.; Desta, I. T.; Naumov, P. Shape-Memory and Self-Healing Effects in Mechanosalient Molecular Crystals. *J. Am. Chem. Soc.* **2016**, *138*, 13298-13306.

(27) Panda, M. K.; Runčevski, T.; Husain, A.; Dinnebier, R. E.; Naumov, P. Perpetually Self-Propelling Chiral Single Crystals. *J. Am. Chem. Soc.* **2015**, *137*, 1895-1902.

(28) Rath, B. B.; Gallo, G.; Dinnebier, R. E.; Vittal, J. J. Reversible Thermosalience in a One-Dimensional Coordination Polymer Preceded by Anisotropic Thermal Expansion and the Shape Memory Effect. *J. Am. Chem. Soc.* **2021**, *143*, 2088-2096

(29) Panda, M. K.; Runčevski, T.; Chandra Sahoo, S.; Belik, A. A.; Nath, N. K.; Dinnebier, R. E.; Naumov, P. Colossal Positive and Negative Thermal Expansion and Thermosalient Effect in a Pentamorphic Organometallic Martensite. *Nat. Commun.* **2014**, *5*, 1-8.

(30) Chen, Y.; Li, J.; Gong, J., Jumping Crystal Based on an Organic Charge Transfer Complex with Reversible ON/OFF Switching of Luminescence by External Thermal Stimuli. *ACS Materials Lett.* **2021**, *3*, 275-281.

Additional Issues

Additional issues are some points not mentioned in the manuscript while discussed with the reviewers.

1. **Oak ridge thermal ellipsoid plot diagrams** (C: black, N: blue, O: red, and S: yellow):

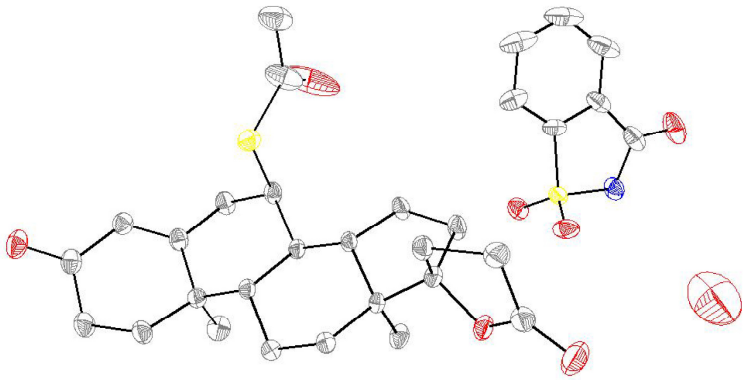

Figure S12. Oak ridge thermal ellipsoid plot diagram of SPI-SAC-0.5H_2O at 113 K.

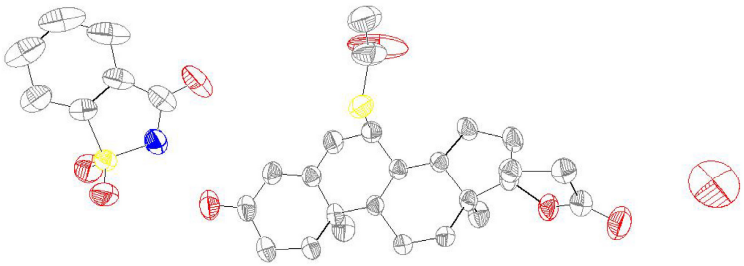

Figure S13. Oak ridge thermal ellipsoid plot diagram of SPI-SAC-0.5H_2O at 298 K.

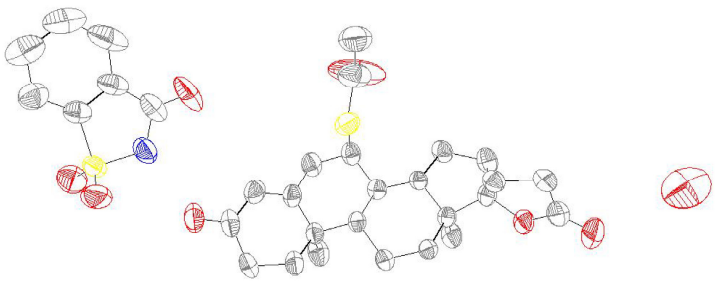

Figure S14. Oak ridge thermal ellipsoid plot diagram of SPI-SAC-0.25H_2O at 353 K.

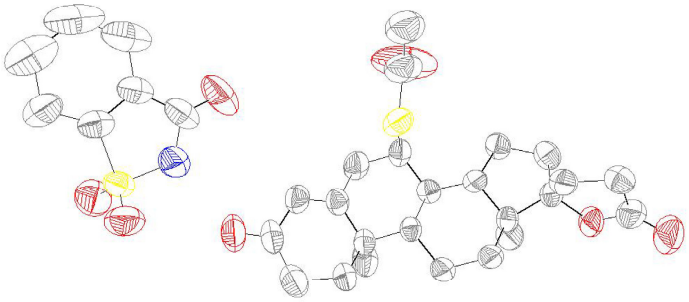

Figure S15. Oak ridge thermal ellipsoid plot diagram of SPI-SAC at 393 K.

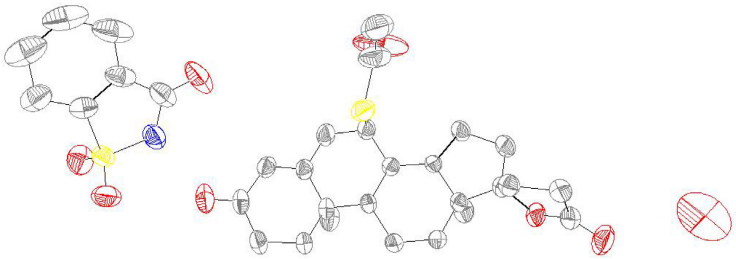

Figure S16. Oak ridge thermal ellipsoid plot diagram of SPI-SAC-0.125H_2O at 298 K.

Notes: All the hydrogen atoms are omitted for clarity.

2. The description of SPI-SAC hydrate cocrystal structure characteristics

At 298K, there is one SPI and one SAC molecule in the asymmetric unit, which are connected by N─H···O hydrogen bond formed between the ketone group on the six-membered ring of SPI and N─H group on SAC. Further, SPI and SAC molecules are stacked face-to-face along the b-axis to form a three-dimensional structure with 3.7×4.3 Å channels, which were occupied by water molecules bonded with two very weak hydrogen bonds connected with the ketone group on the five-membered ring of SPI.